Buoyancy-forced circulation in an idealized Red Sea

Ping Zhai[1], Amy Bower[2], Larry Pratt[2] | [1]MIT-WHOI Joint Program in Physical Oceanography, Woods Hole, Massachusetts (pingzhai@mit.edu)
[2]Department of Physical Oceanography, Woods Hole Oceanographic Institution, Woods Hole, Massachusetts

1. Introduction

Buoyancy loss in marginal seas, such as the Red Sea, the Mediterranean Sea, the Nordic Seas, the Labrador Sea and the Weddell Sea can produce dense intermediate and deep water which feed the deep branch of the thermohaline circulation. Therefore, understanding the transformation mechanism of the water masses in the marginal seas is important in studying the global thermohaline circulation.

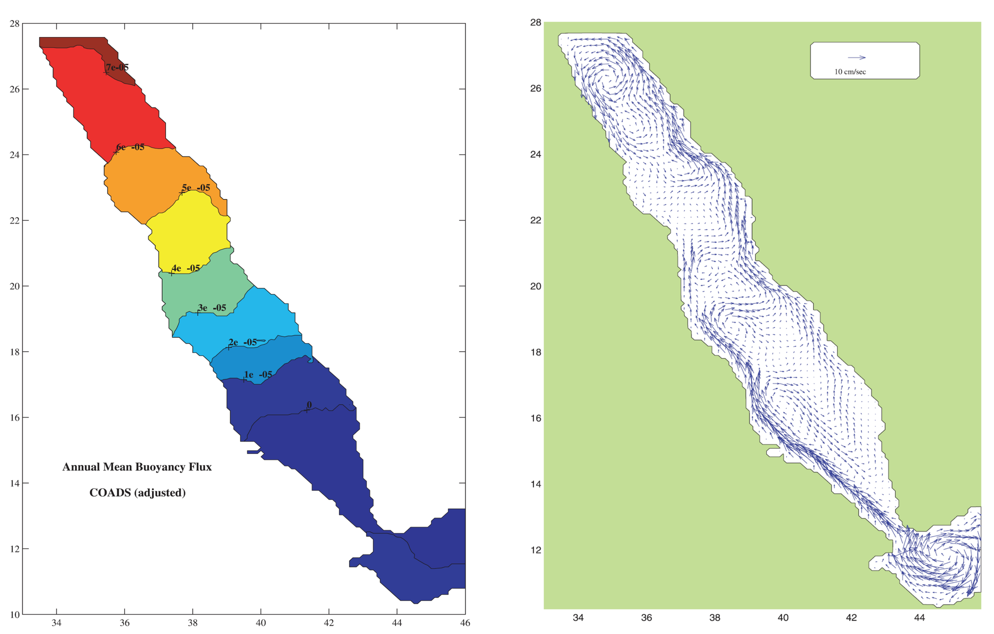

Figure 1. Left: Annual mean buoyancy loss over the Red Sea (in kg/m/s^3), using the COADS climatology. The buoyancy loss increases from 0 in the southern Red Sea to 7×10^{-5} in the northern Red Sea. Right: Sea surface velocity driven by the buoyancy loss (Figure 1 and 15 of Sofianos et al., 2003).

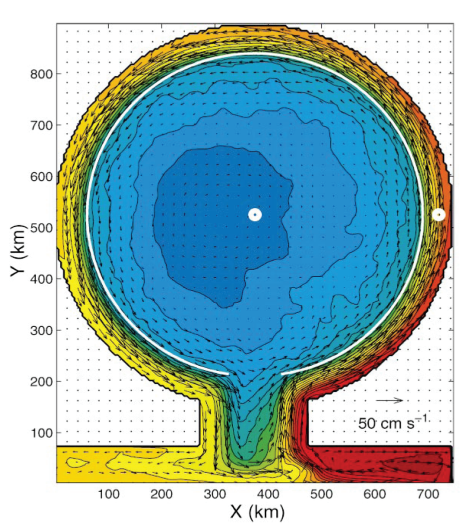

Figure 2. Mean upper level temperature and horizontal velocity (Figure 2 in Spall (2004)). Buoyancy is horizontally uniform and f is constant in Spall's model.

The objective of this study is to understand what controls the water mass transformation and crossover latitude of the northward western boundary current by using MITgcm and an analytical model.

Conclusions:

1. The crossover latitude increases when we increase β, or decrease f_0, or increase the meridional gradient of the buoyancy forcing.
2. The crossover latitude is well predicted by the analytical model.
3. The competition between the plantary PV term and the stretching PV term determines the crossover latitude. South of the crossover latitude, planatary PV dominates the PV advection, while north of the crossover latitude, stretching PV dominates.

2. Numerical model description and results

The buoyancy driven circulation in the idealized Red Sea is explored using MITgcm. In the idealized model, the Red Sea is a 300 km wide and 1600 km long rectangular basin. The bottom slopes downward from 0 to 1000 m at a distance 80 km. β-plan is used in the simulation.

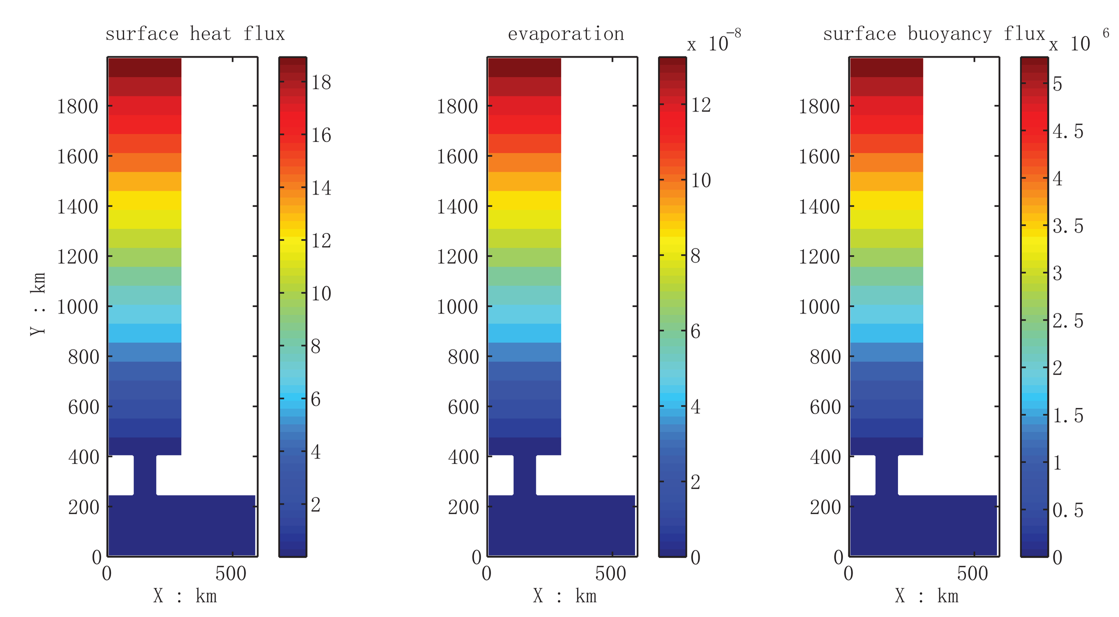

Figure 3. Surface heat loss (left, in W/m^2), evaporation rate (middle, in m/s) and buoyancy loss (right, in kg/m^2/s) that drive the circulation in the idealized Red Sea in the control run (EXP0).

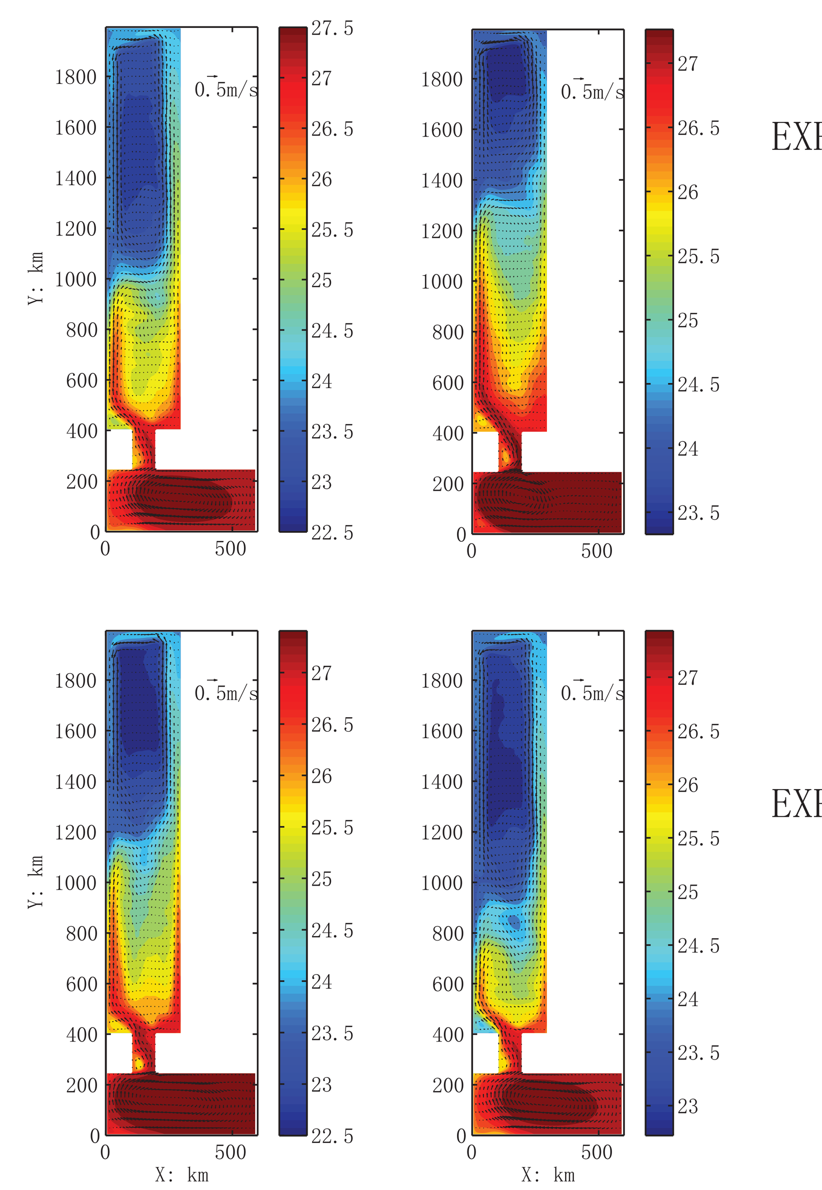

Figure 4. The mean surface zonal velocity and temperature averaged over the final 5 years of a 25-year simulation. The results of EXP0, EXP3, EXP8 and EXP11 are shown here.

References:

Spall, Michael A., 2004: Boundary Currents and Watermass Transformation in Marginal Seas. J. Physi. Oceanogr., 34, 1197 - 1213.

Sofianos, S. S., and W. E. Johns, 2003: An Oceanic General Circulation Model (OGCM) investigation of the Red Sea circulation: 2. Three-dimensional circulation in the Red Sea. J. Geophys. Res., 108(C3), 3066, doi:10.1029/2001JC001185.

Acknowledgement:

This work is supported by Award Nos. USA 00002, KSA 00011 and KSA 00011/02 made by King Abdullah University of Science and Technology (KAUST) and National Science Foundation OCE0927017 .

3. Analytical model-estimate the boundary current density

An analytical model is developed to explore what determines the crossover latitude of the northward western boundary current. The motion in the numerical model confines in the upper 200 m (H). The analytical model is very idealized and we assume that the velocity in the upper 200 m is constant and zero below 200 m.

$$0=-u\frac{\partial q}{\partial x}-v\frac{\partial q}{\partial y}-r\zeta$$

$$q=\beta y-\frac{f_0 g}{\rho_0}\frac{\partial}{\partial z}\frac{\rho'}{N^2}$$

$$\zeta=\frac{\partial v}{\partial x}-\frac{\partial u}{\partial y}$$

$$\iint_A\left[u_1\frac{\partial}{\partial x}\left(\beta y-\frac{2f_0 g}{\rho_0 H}\frac{\rho_1'}{N^2}\right)+v_1\frac{\partial}{\partial y}\left(\beta y-\frac{2f_0 g}{\rho_0 H}\frac{\rho_1'}{N^2}\right)\right]dxdy=-rc_1$$

$$c_1=\oint_C \vec{v_1}\cdot\vec{dl}$$

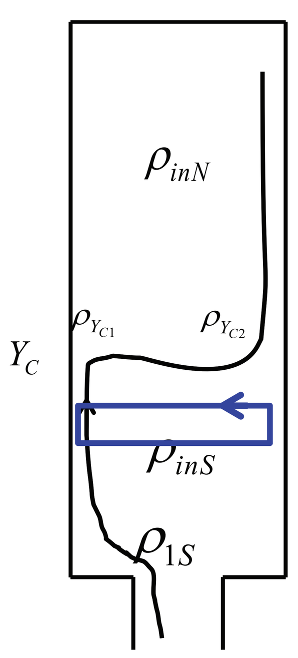

$$\frac{d\rho_1}{ds}=\frac{B_0/H}{v_1}$$

b. At y=Yc

$$u_1=\frac{Hg}{2\rho_0(f_0+\beta Y_C)}\frac{\rho_{inN}-\rho_{inS}}{L}$$

$$\rho_1=\rho_{Y_{C1}}-\int_{x_W}^{x}\frac{2LB_0\rho_0(f_0+\beta Y_C)}{H^2 g(\rho_{inN}-\rho_{inS})}dy$$

a. South of Yc

$$v_1=\frac{Hg}{2\rho_0(f_0+\beta y)}\frac{\rho_1-\rho_{inS}}{L}$$

$$\rho_1^2-2\rho_{inS}\rho_1-\left(\rho_{1S}^2-2\rho_{inS}\rho_{1S}\right)-2F=0$$

$$F(y)=\int_{y=y_S}^{y}\frac{2B_0 f\rho_0 L}{H^2 g}dy$$

$$\rho_{inS}-\rho_{bS}=-\sqrt{\frac{WB_{TS}\rho_0 f_0}{2cH^2 g(W+L_{0S})}}$$

$$B_T=\int_{y_S}^{Y_C}B_0 dy$$

$$\rho_1=\rho_{inS}+\left(\rho_S-\rho_{inS}\right)\sqrt{1+\frac{2F}{\left(\rho_{inS}-\rho_S\right)^2}}$$

c. North of Yc

$$v_1=-\frac{Hg}{2\rho_0(f_0+\beta y)}\frac{\rho_1-\rho_{inN}}{L}$$

$$\rho_1^2-2\rho_{inN}\rho_1-\left(\rho_{Y_{C2}}^2-2\rho_{inN}\rho_{Y_{C2}}\right)+2F=0$$

$$F(y)=\int_{y=Y_C}^{y}\frac{2B_0 f\rho_0 L}{H^2 g}dy$$

$$\rho_{inN}-\rho_{bN}=\sqrt{\frac{WB_{TN}\rho_0 f_0}{2cH^2 g(W+L_{0N})}}$$

$$B_T=\int_{Y_C}^{Yn}B_0 dy$$

$$\rho_1=\rho_{inN}-\left(\rho_{inN}-\rho_{Y_{C2}}\right)\sqrt{1-\frac{2F}{\left(\rho_{inN}-\rho_{Y_{C2}}\right)^2}}$$

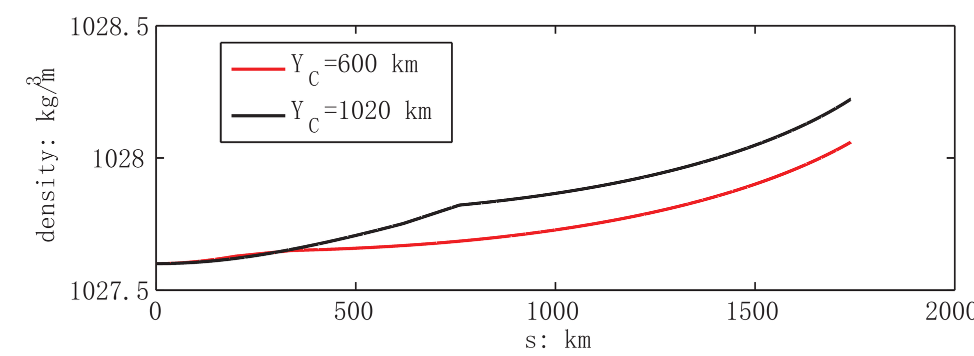

Figure 5. Analytical solution of the density along the pathway. Results of two different Y_C are shown. β, f_0 and surface buoyancy forcing used here is the same as numerical model EXP0.

Table 1: Model run parameters and symbols used in Figure 9. ay+b=B_0 is the surface buoyancy flux.

	f_0	β	a	b	symbol
EXP0	3.5×10^{-5}	2.1×10^{-11}	3.5×10^{-12}	-1.4×10^{-6}	Δ
EXP3	1.5×10^{-5}	2.1×10^{-11}	3.5×10^{-12}	-1.4×10^{-6}	•
EXP4	2.5×10^{-5}	2.1×10^{-11}	3.5×10^{-12}	-1.4×10^{-6}	•
EXP5	7×10^{-5}	2.1×10^{-11}	3.5×10^{-12}	-1.4×10^{-6}	•
EXP6	10.5×10^{-5}	2.1×10^{-11}	3.5×10^{-12}	-1.4×10^{-6}	•
EXP7	3.5×10^{-5}	1.5×10^{-11}	3.5×10^{-12}	-1.4×10^{-6}	Δ
EXP8	3.5×10^{-5}	4×10^{-11}	3.5×10^{-12}	-1.4×10^{-6}	Δ
EXP9	3.5×10^{-5}	6×10^{-11}	3.5×10^{-12}	-1.4×10^{-6}	Δ
EXP10	3.5×10^{-5}	2.1×10^{-11}	0	2.8×10^{-6}	O
EXP11	3.5×10^{-5}	2.1×10^{-11}	1.7×10^{-12}	0.7×10^{-6}	O
EXP12	3.5×10^{-5}	2.1×10^{-11}	2.6×10^{-12}	-0.34×10^{-6}	O
EXP13	3.5×10^{-5}	2.1×10^{-11}	4.3×10^{-12}	-2.4×10^{-6}	O

4. Analytical model-determine the crossover latitude

According to the PV balance equation, positive PV advection requires anticyclonic circulation while negative PV advection requires cyclonic circulation.

$$L\int_{y}^{y+1km}v_1\frac{\partial}{\partial y}\left(\beta y-\frac{2f_0 g}{\rho_0 H}\frac{\rho_1'}{N^2}\right)dy=-rc_1$$

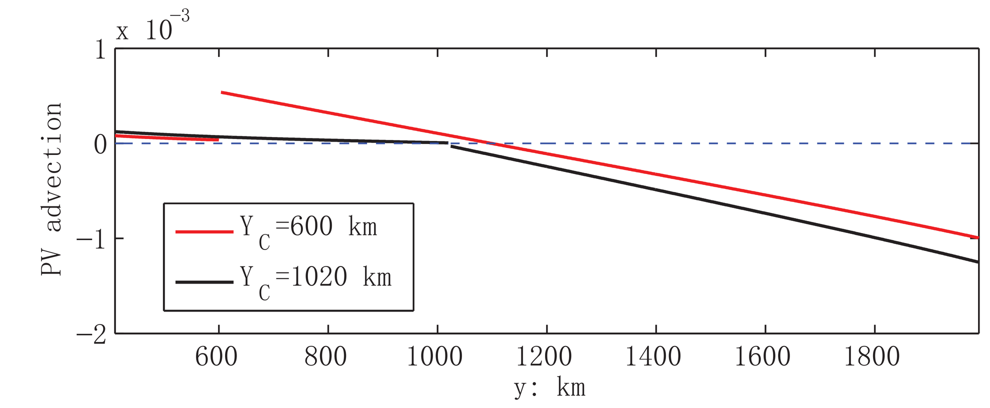

Figure 6. PV advection in the PV balance equation. Parameters are the same as in Figure 5. If Yc=600 km, the PV balance equation implies that south of 1100 km, the circulation should be anticyclonic. It has been assumed that north of 600 km, the circulation is cyclonic. Therefore, 600 km is not the correct crossover latitude.

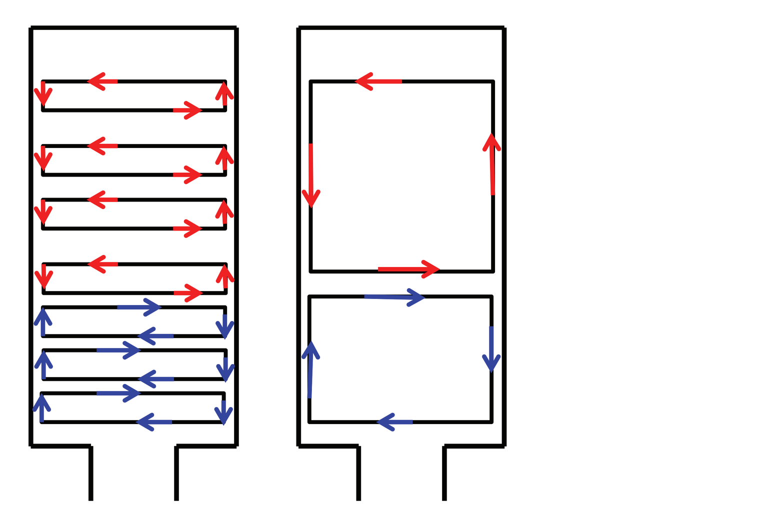

Figure 7. Schematics illustrating how circulation is determined according to PV balance.

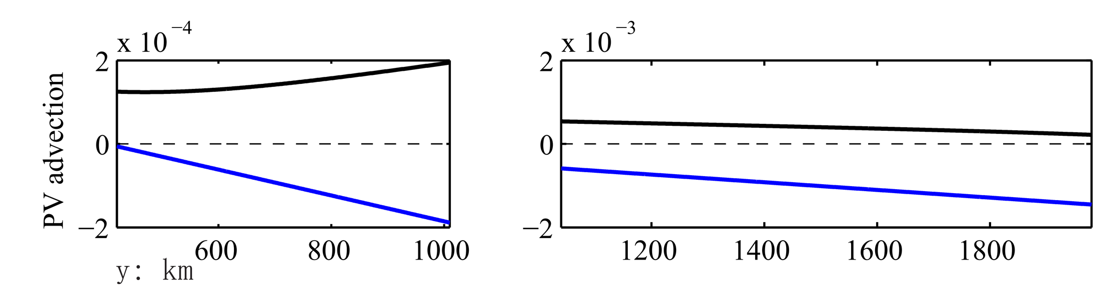

Figure 8. PV advection due to planetary PV term (black) and stretching PV term (blue) respectively.

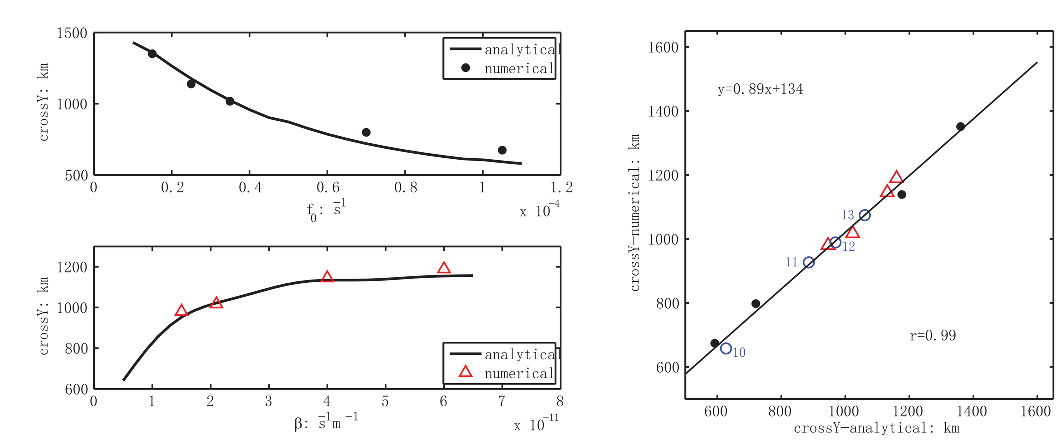

Figure 9. Comparison between the analytical model and a series of numerical models.